

Update on B_K and ε_K with staggered quarks

Taegil Bae, Yong-Chull Jang, Hwancheol Jeong, Jangho Kim, Jongjeong Kim, Kwangwoo Kim, Seonghee Kim, Weonjong Lee*, Jaehoon Leem, Jeonghwan Pak, Sungwoo Park

*Lattice Gauge Theory Research Center, CTP, and FPRD,
Department of Physics and Astronomy, Seoul National University, Seoul, 151-747, South Korea
E-mail: wlee@snu.ac.kr*

Chulwoo Jung, Hyung-Jin Kim

*Physics Department, Brookhaven National Laboratory, Upton, NY11973, USA
E-mail: chulwoo@bnl.gov*

Stephen R. Sharpe

*Physics Department, University of Washington, Seattle, WA 98195-1560, USA
E-mail: sharpe@phys.washington.edu*

Boram Yoon

*Los Alamos National Laboratory,
Theoretical Division T-2, MS B283,
Los Alamos, NM 87545, USA
E-mail: googlus@gmail.com*

SWME Collaboration

We update our results for B_K obtained using HYP-smeared staggered valence quarks on the MILC asqtad lattices. In the last year, we have added 5 new measurements on the fine ($a \approx 0.09$ fm) ensembles, and 2 new measurements on the superfine ($a \approx 0.06$ fm) ensembles. These allow a simultaneous extrapolation in a^2 and sea quark masses, reducing the corresponding systematic error significantly. Our updated result is $\hat{B}_K = 0.738 \pm 0.005(\text{stat}) \pm 0.034(\text{sys})$.

31st International Symposium on Lattice Field Theory - LATTICE 2013

July 29 - August 3, 2013

Mainz, Germany

*Speaker.

1. Introduction

The standard model prediction for ε_K is proportional to the kaon mixing matrix element parametrized by B_K . Recent progress in the calculation of B_K and other quantities using lattice QCD [1] allows a high-precision test of the standard model. Although B_K is a subdominant source of error in present estimates of ε_K , this may well change in the future, so further reduction in the errors is worthwhile.

Here we update the determination of B_K using improved staggered quarks. At Lattice 2012, we found the surprising result that the slope of B_K versus light sea-quark mass depended non-monotonically on the lattice spacing (see Fig. 3 of Ref. [2]). To investigate further, we have added 7 new lattice ensembles with different values of the sea-quark masses (see Table 1). This has resolved last year's problem, as described below.

Table 1 lists all the MILC asqtad ensembles on which we have calculated (or are calculating) B_K . In our earlier calculations, we used only a subset of these ensembles. Initially, we took the continuum limit using ensembles F1, S1 and U1 (i.e. holding the ratio of light to strange sea-quark masses fixed), while estimating the sea-quark mass dependence from the coarse lattice ensembles C1-C5 [3]. By Lattice 2012, we had added ensembles F2, F3, S2 and S3 (and increased statistics on several ensembles) [2]. Since then we have added measurements on ensembles F4, F5, F6, F7, F9, S4 and S5 (with F8 and S6 in the pipeline). The net effect is that we can study the sea-quark mass dependence in much greater detail, and in particular do a combined continuum, light sea-quark mass and strange sea-quark mass extrapolation.

2. Valence quark mass extrapolations

We used a mixed action, with asqtad sea quarks and HYP-smeared [4] valence quarks. We denote the masses of the valence d and s quarks by m_x and m_y , respectively, while the light and strange sea-quark masses are m_ℓ and m_s . On each ensemble, we use 10 valence masses: $am_x, am_y = am_s^{\text{nom}} \times (n/10)$ with $n = 1, 2, 3, \dots, 10$, where $am_s^{\text{nom}} = 0.05, 0.030, 0.018$ and 0.014 on the coarse, fine, superfine and ultrafine ensembles, respectively. We extrapolate to the physical value of m_d using the lightest four values of m_x , and to the physical m_s using the heaviest three m_y . We are then in the regime ($m_x \ll m_y \sim m_s$) where SU(2) [staggered] chiral perturbation theory ([S]ChPT) is applicable.

We call the extrapolation in m_x the “X-fit”. We fit to the next-to-leading order (NLO) SChPT finite-volume form worked out in Refs. [5, 6], augmented by NNLO and higher order terms, including Bayesian constraints, as described in Refs. [6, 3]. Examples of these fits for two of the new ensembles are shown in Fig. 1. These are the ensembles with the lightest light sea quarks at the “fine” ($a \sim 0.09$ fm) and “superfine” ($a \sim 0.06$ fm) lattice spacings. Indeed, on ensemble F9 our sea quarks have $m_\ell = m_s/20$, which is lighter than our lightest valence quark, and corresponds to a sea-quark pion of mass ~ 180 MeV. In the figures, the red diamond is the value obtained after extrapolating to $m_x = m_d$, setting the pion masses appearing in the NLO chiral logarithms to their physical values (with taste-breaking removed) and setting the volume to infinity. Systematic errors in the X-fits are estimated by varying the Bayesian priors and by using fits with and without NNNLO terms.

a (fm)	am_l/am_s	geometry	ID	ens \times meas	status
0.12	0.03/0.05	$20^3 \times 64$	C1	564×9	old
0.12	0.02/0.05	$20^3 \times 64$	C2	486×9	old
0.12	0.01/0.05	$20^3 \times 64$	C3	671×9	old
0.12	0.01/0.05	$28^3 \times 64$	C3-2	275×8	old
0.12	0.007/0.05	$20^3 \times 64$	C4	651×10	old
0.12	0.005/0.05	$24^3 \times 64$	C5	509×9	old
0.09	0.0062/0.0186	$28^3 \times 96$	F6	950×9	new
0.09	0.0124/0.031	$28^3 \times 96$	F4	1995×9	new
0.09	0.0093/0.031	$28^3 \times 96$	F3	949×9	old
0.09	0.0062/0.031	$28^3 \times 96$	F1	995×9	old
0.09	0.00465/0.031	$32^3 \times 96$	F5	651×9	new
0.09	0.0031/0.031	$40^3 \times 96$	F2	959×9	old
0.09	0.0031/0.0186	$40^3 \times 96$	F7	701×9	new
0.09	0.0031/0.0031	$40^3 \times 96$	F8	576×9	NA
0.09	0.00155/0.031	$64^3 \times 96$	F9	790×9	new
0.06	0.0072/0.018	$48^3 \times 144$	S3	593×9	old
0.06	0.0054/0.018	$48^3 \times 144$	S4	582×9	new
0.06	0.0036/0.018	$48^3 \times 144$	S1	749×9	old
0.06	0.0025/0.018	$56^3 \times 144$	S2	799×9	old
0.06	0.0018/0.018	$64^3 \times 144$	S5	821×6	new
0.06	0.0036/0.0108	$64^3 \times 144$	S6	600×0.05	NA
0.045	0.0028/0.014	$64^3 \times 192$	U1	747×1	old

Table 1: MILC asqtad ensembles used to calculate B_K . am_l and am_s are the masses, in lattice units, of the light and strange sea quarks, respectively. “ens” indicates the number of configurations on which “meas” measurements are made. Note that the numbering of the ID tags on the fine and superfine lattices do not follow the ordering of am_l . “NA” means that analysis results are not yet available.

The extrapolation of m_y to the physical m_s (the “Y-fit”) is done using linear and quadratic fits. The quadratic terms are very small, as in our earlier work [3, 6]. We use the linear fits for the central value and the quadratic fits to estimate a systematic error.

3. Continuum Extrapolation

At this stage, we have one-loop matched results for $B_K(1/a)$ on each ensemble. We first run these to a common scale, which we take to be 2 GeV. The remaining errors are those due to discretization (primarily taste-conserving), the need to extrapolate in the sea-quark masses m_l and m_s , and truncation errors in the matching factors. Note that the sea-quark mass dependence is analytic at NLO, because we have accounted for the chiral logarithms in the valence-quark extrapolations.

With our much enlarged data-set, it is now possible to perform a simultaneous fit to a^2 , m_l and m_s , which is a significant improvement compared to our previous work. We have tried a number of fit functions, but discuss here only the simplest and most complicated forms, which we label B1

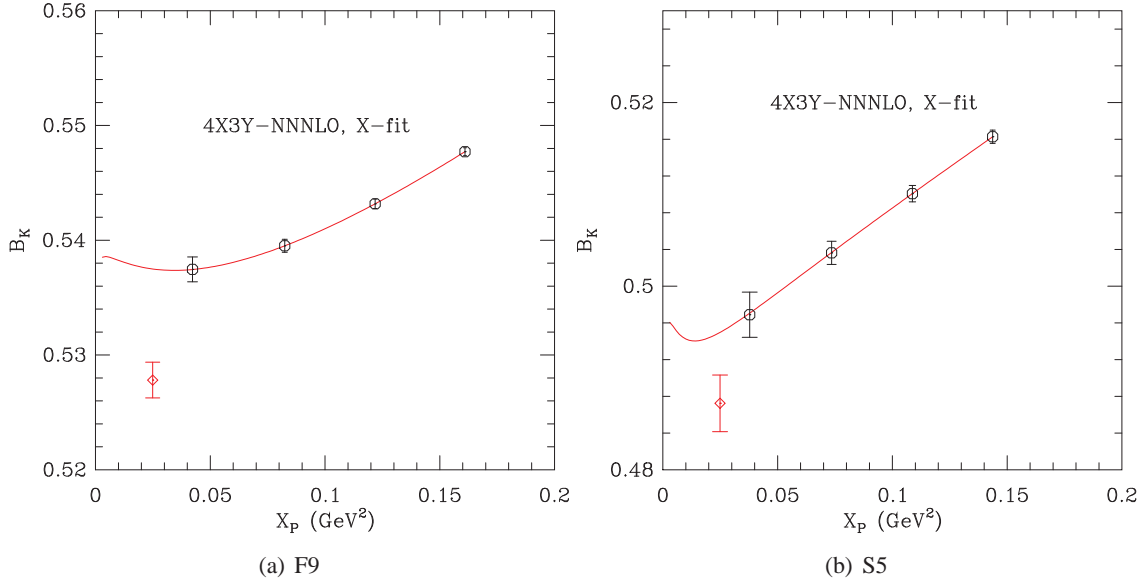


Figure 1: X-fits to $B_K(1/a)$ for the F9 and S5 ensembles. Here X_P is the mass of the $x\bar{x}$ valence taste- ξ_5 pion. The red diamond is explained in the text.

and B4, respectively. The B1 fit function is

$$f_{B1} = c_1 + c_2(a\Lambda_Q)^2 + c_3 \frac{L_P}{\Lambda_X^2} + c_4 \frac{S_P}{\Lambda_X^2}. \quad (3.1)$$

with L_P (S_P) the squared pion masses of the taste- ξ_5 $\ell\bar{\ell}$ ($s\bar{s}$) pions. The scales are chosen to be $\Lambda_Q = 0.3$ GeV and $\Lambda_X = 1.0$ GeV, with Bayesian constraints $c_i = 0 \pm 2$ for $i = 2, 3, 4$. This forces the parameters to have magnitudes similar to those expected from dimensional analysis. The linear dependence on L_P is the prediction of NLO SchPT, while that on S_P is just the simplest choice for a smooth function.

We show the B1 fit in Fig. 2. Although results from the coarse ensembles C1-C5 are displayed, they are not included in the fit. Doing so leads to very low confidence levels for all fit forms we have tried. Thus we include in the fit only the 8 fine, 5 superfine and 1 ultrafine ensembles, and find a reasonable fit with $\chi^2/\text{dof} = 1.46$. We note that the fine and superfine points should not lie precisely on the corresponding lines shown in the plots, because their values for a^2 and S_P vary slightly (by up to 6% and 3%, respectively). This discrepancy is much larger for ensembles F6 and F7, which have significantly different values of am_s , and so we do not display the results from these two ensembles (although they are included in the fit). These ensembles give us a strong “lever-arm” for determining the S_P dependence. We stress that we do not build in SU(3) symmetry— c_3 and c_4 are independent parameters, and indeed turn out to differ significantly.

The B4 fit uses the form

$$f_{B4} = f_{B1} + c_5(a\Lambda_Q)^2 \frac{L_P}{\Lambda_X^2} + c_6(a\Lambda_Q)^2 \frac{S_P}{\Lambda_X^2} + c_7[\alpha_s(\frac{1}{a})]^2 + c_8(a\Lambda_Q)^2 \alpha_s(\frac{1}{a}) + c_9(a\Lambda_Q)^4 \quad (3.2)$$

The most significant new term is that proportional to α_s^2 , since this varies the most slowly with a . This term is present because we use one-loop matching. All the new terms are constrained along

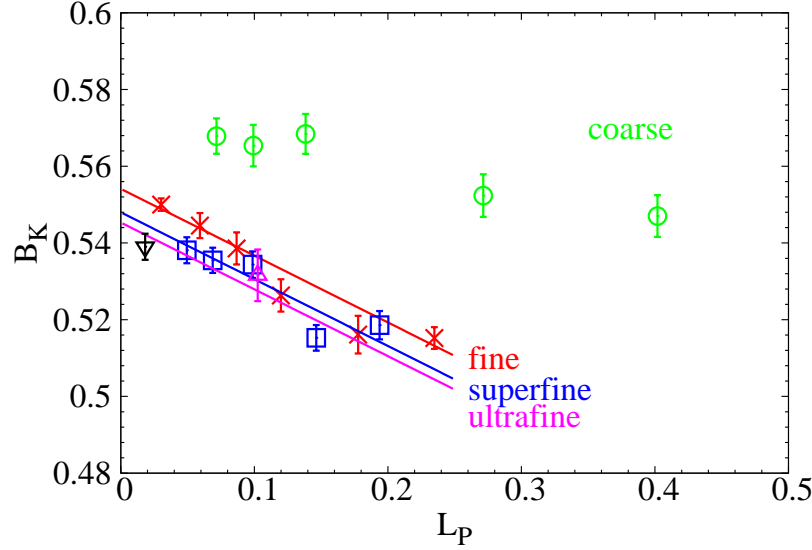


Figure 2: $B_K(\mu = 2 \text{ GeV})$ vs. $L_P (\text{GeV}^2)$ with a B1 fit. The black diamond is result at $a = 0$ and with physical sea-quark masses. The lines show the fit function with a^2 and S_P fixed to the average value for the corresponding ensembles (fine, superfine or ultrafine), except that for the fine ensembles S_P is the average of the values on ensembles F1, F2 and F4.

the lines described above. The result of the B4 fit is shown in Fig. 3. The quality of fit barely changes from the B1 fit, with χ^2/dof still 1.46. The main change in the B4 fit is an increase in the statistical error (as we expect with more parameters), along with a shift in the central value which is not statistically significant. We see that the data neither “wants” nor excludes the extra terms in the fit function. Nevertheless, since the extra terms are theoretically well motivated, we use the difference between the results of the B4 and B1 fits as our estimate of the systematic error in the continuum-chiral extrapolation, while using B1 for the central value.

As mentioned in the introduction, our results last year showed a non-monotonicity in the dependence of the slopes versus L_P as we approached the continuum limit. Comparing to Fig. 3 of Ref. [2], we find that two factors contribute to the resolution of this problem. First, adding more values of L_P allows the slopes to be better determined, and we then find that they are consistent with monotonic dependence on a . Second, we allow for independent L_P and S_P dependence, and account for the variation in a^2 and S_P between ensembles.

4. Final Result and Outlook

After extrapolation we find

$$\hat{B}_K = 0.738 \pm 0.005(\text{stat}) \pm 0.034(\text{sys}) \quad (4.1)$$

The sources of error and their contributions are collected in Table 2. Our methods for estimating the main systematic errors have been described above,¹ with the exception of the matching factor

¹We estimate minor errors following the methods described in Ref. [6].

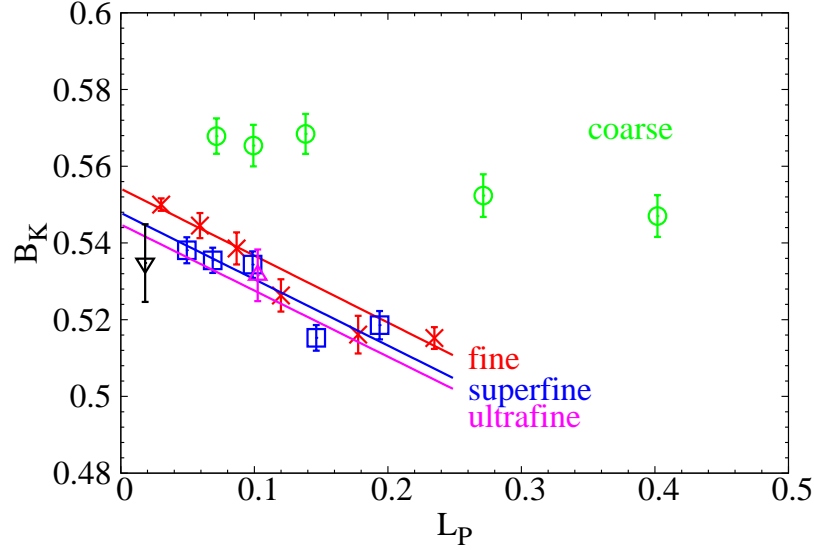


Figure 3: $B_K(\mu = 2 \text{ GeV})$ vs. $L_P (\text{GeV}^2)$ with fit function B4.

error. The latter arises from truncating the perturbative matching factor at one-loop order. We estimate the resulting error as $\Delta B_K/B_K = \alpha_s^2$ with α_s evaluated at scale $1/a$ on the finest (U1) lattice. We note that the difference between B4 and B1 fits includes, in part, an estimate of this truncation error. Thus, when we combine all errors in quadrature, there is some double counting. This is numerically a small effect, however, and we ignore it.

cause	error (%)	memo
statistics	0.63	see text
matching factor	4.4	$\Delta B_K^{(2)} (\text{U1})$
$\left\{ \begin{array}{l} \text{discretization} \\ am_\ell \text{ extrap} \\ am_s \text{ extrap} \end{array} \right\}$	1.1	diff. of B1 and B4 fits
X-fits	0.33	varying Bayesian priors (S1)
Y-fits	0.53	diff. of linear and quad. (F1)
finite volume	0.5	diff. of $V = \infty$ and FV fit [7]
r_1	0.27	r_1 error propagation (F1)
f_π	0.4	132 MeV vs. 124.4 MeV

Table 2: Error budget for B_K using SU(2) SchPT fitting.

Our final result is completely consistent with that we found previously using many fewer ensembles (C1-5, F1, S1 and U1), namely $\hat{B}_K = 0.727(4)(38)$ [3]. The extra ensembles have led to a substantial reduction in the errors from continuum and sea-quark mass extrapolations: this error was previously 2.7% and is now 1.1%. This improvement only leads to a small reduction in the total systematic error, however, due to the dominant (and unchanged) matching error.

As in Ref. [8], we can convert the above results into predictions for ε_K . Preliminary results² are

$$|\varepsilon_K| = 1.51(18) \times 10^{-3} \quad \text{for exclusive } V_{cb} \quad (4.2)$$

$$|\varepsilon_K| = 1.91(21) \times 10^{-3} \quad \text{for inclusive } V_{cb}. \quad (4.3)$$

The former value lies 4σ away from the experimental value $|\varepsilon_K| = 2.228(11) \times 10^{-3}$.

Further improvement clearly requires reducing the matching factor error. To do so we are calculating the matching factors using non-perturbative renormalization (NPR) in the RI-MOM and RI-SMOM schemes. Preliminary results (for bilinears) are reported in Ref. [10]. See also Ref. [11]. We expect that NPR will reduce the error in matching down to the $\sim 2\%$ level. We are also pursuing a two-loop perturbative matching calculation.

5. Acknowledgments

We are grateful to Claude Bernard and the MILC collaboration for private communications. C. Jung is supported by the US DOE under contract DE-AC02-98CH10886. The research of W. Lee is supported by the Creative Research Initiatives Program (2013-003454) of the NRF grant funded by the Korean government (MSIP). W. Lee would like to acknowledge the support from KISTI supercomputing center through the strategic support program for the supercomputing application research [No. KSC-2012-G3-08]. The work of S. Sharpe is supported in part by the US DOE grant no. DE-FG02-96ER40956. Computations were carried out in part on QCDOC computing facilities of the USQCD Collaboration at Brookhaven National Lab, on GPU computing facilities at Jefferson Lab, on the DAVID GPU clusters at Seoul National University, and on the KISTI supercomputers. The USQCD Collaboration is funded by the Office of Science of the U.S. DOE.

References

- [1] G. Colangelo, S. Durr, A. Juttner, L. Lellouch, H. Leutwyler, *et al.* *Eur.Phys.J.* **C71** (2011) 1695, [arXiv:1011.4408].
- [2] **SWME** Collaboration, T. Bae *et al.* *PoS LATTICE2012* (2012) 274, [arXiv:1211.1545].
- [3] T. Bae *et al.* *Phys.Rev.Lett.* **109** (2012) 041601, [1111.5698].
- [4] A. Hasenfratz and F. Knechtli, *Flavor symmetry and the static potential with hypercubic blocking*, *Phys.Rev.* **D64** (2001) 034504, [hep-lat/0103029].
- [5] R. S. Van de Water and S. R. Sharpe *Phys.Rev.* **D73** (2006) 014003, [hep-lat/0507012].
- [6] T. Bae, Y.-C. Jang, C. Jung, H.-J. Kim, J. Kim, *et al.* *Phys.Rev.* **D82** (2010) 114509, [1008.5179].
- [7] J. Kim, C. Jung, H.-J. Kim, W. Lee, and S. R. Sharpe *Phys.Rev.* **D83** (2011) 117501, [arXiv:1101.2685].
- [8] Y.-C. Jang and W. Lee *PoS LATTICE2012* (2012) 269, [arXiv:1211.0792].
- [9] Y.-C. Jang, W. Lee, *et al.* *in preparation*.
- [10] J. Kim, J. Kim, W. Lee, and B. Yoon arXiv:1310.4269.
- [11] A. T. Lytle and S. R. Sharpe *Phys.Rev.* **D88** (2013) 054506, [1306.3881].

²The final results will be reported in Ref. [9].